PCCP

Accepted Manuscript

ROYAL SOCIETY OF CHEMISTRY

www.rsc.org/pccp

Stiffness and Evolution of Interfacial Micropancakes Revealed by AFM Quantitative Nanomechanical Imaging

Binyu Zhao, [1,2] Xingya Wang, [1, 2,3] Yang Song, [1,2] Jun Hu, [1,2] Junhong Lü, [1,2] Xingfei Zhou, [3] Renzhong Tai, [1, 2,5] Xuehua Zhang, [4,*] and Lijuan Zhang, [1, 2,5,*]

[1] Shanghai Institute of Applied Physics, Chinese Academy of Sciences, Shanghai 201800, China

[2] Key Laboratory of Interfacial Physics and Technology, Chinese Academy of Sciences

[3] Department of Physics, Ningbo University, Ningbo 315211, China

[4] School of Civil, Environmental and Chemical Engineering, RMIT University, Melbourne, VIC 3001, Australia

[5] Shanghai Synchrotron Radiation Facility, Shanghai 201204, China

*Correspondence to [xuehua.zhang@rmit.edu.au] or [zhanglijuan@sinap.ac.cn]

Abstract

Micropancakes are quasi-two-dimensional micron-sized domains on crystalline substrates (e.g. highly oriented pyrolytic graphite (HOPG)) immersed in water. They are only a few nanometers in their thickness, and are suspected to come from the accumulation of dissolved air at the solid-water interface. However, the exact chemical nature and basic physical properties of micropancake are on debate ever since their first observation, primarily due to lack of a suitable characterization technique. In this study, the stiffness of micropancakes at the interface between HOPG and ethanol/water solutions was investigated by using PeakForce Quantitative NanoMechanics (PF-QNM) mode Atomic Force Microscopy (AFM). Our measurements showed that micropancakes were stiffer than nanobubbles, and for bilayer micropancakes, the bottom layer in contact with the substrate was stiffer than the top one. Interestingly, the micropancakes became smaller and softer with an increase in the ethanol concentration in the solution, and were undetectable by AFM above a critical concentration of ethanol. But they re-appeared after the ethanol concentration in the solution was reduced. Clearly the evolution and stiffness of the micropancakes were dependent on the chemical composition in the solution, which could be attributed to the correlation of the mechanical properties of the micropancakes to the surface tension of the liquid phase. Based on the "go-and-come" behaviors of micropancakes with the ethanol concentration, we found that the micropancakes could actually tolerate the ethanol concentration much higher than 5%, a value reported in literature. The results from this work may be helpful in alluding the chemical nature of micropancakes.

1. INTRODUCTION

In last two decades, accumulated gases at water-hydrophobic solid interfaces attracted increasing attention from many researchers. The claimed forms of the accumulated interfacial gaseous domains include nanobubbles,[1-12] micropancakes,[13-19] interfacial gas enrichment layer,[20-22] water depletion layer,[23-26] and, very recently, cap-shaped nanostructures, pancake-shaped disordered layers, and ordered epitaxial layers.[27-30] Among them, the micropancakes are flat, quasi-two-dimensional, pancake-like domains at the interface between a solid substrate and water. Their lateral length scale spans from a few tens of nanometers to several microns, while their apparent thickness measured from the tapping mode atomic force microscopy images is generally less than 3 nm. Direct experimental observation of the micropancakes was first reported by Zhang et al.[13] on highly oriented pyrolytic graphite (HOPG) surface in contact with water. Later, multiple layers (bilayers micropancakes and nanobubble-on-bilayer micropancakes) were also found at the water/HOPG interface.[15] Besides on the HOPG surface, micropancakes have also been observed on other crystalline surfaces in water including talc and MoS_2.[13, 16]

The exact chemical nature of such micropancakes still remains puzzling. Some researches proposed that micropancakes comprised dense gas adsorbates based on the degassing effects[8, 9], however, no direct experimental evidence has been reported so far to reveal their gaseous nature unambiguously. It also remains unknown what are the basic mechanical properties (stiffness) of micropancakes. One may expect that the stiffness of such thin layers may be coupled with the substrate properties, together with the thickness and the liquid-gas interfacial tension. Even puzzling, it was experimentally observed that a nanobubble may sit on top of micropancakes and the micropancakes may have more than one layer. The systematic investigation on the fundamental properties and stability of micropancakes will be helpful for understanding some of the mysteries associated with micropancakes and other claimed forms of interfacial gaseous domains.[14, 21, 31-33]

However, the direct observation of micropancakes has up to now been restricted to tapping mode AFM, and the known properties are almost limited to the morphologies, insufficient for further analysis.[7-9, 13-19] A serious problem is that the topography imaging sometimes makes it difficult to discriminate the thin micropancakes layers from the substrate steps, while phase imaging just measures a time-average of force or

dissipation over time, making it ambiguous to present the different material properties.[34, 35]

PeakForce Quantitative NanoMechanics (PF-QNM) is a novel direct force-control mode AFM, one of the advantages of which is that not only the morphological but also the quantitative mechanical properties, such as stiffness, adhesion and deformation of materials can be separated and obtained simultaneously with high spatial resolution and presented in different channels.[34, 36] By using PF-QNM, Walczyk et al.[37] and Yang et al.[38] successfully imaged interfacial nanobubbles and constructed their morphological profiles, finding that the morphologies of nanobubbles from low force PF-QNM measurement were comparable to that obtained by tapping mode AFM. In the recent work, we measured the stiffness of nanobubbles quantitatively by the PF-QNM both in pure water and in ethanol/water solutions, demonstrating that the surface tension of nanobubbles is almost equal to the surface tension of the surrounding solutions.[36, 39] In order to provide novel information to understand the physical nature of micropancakes from their stiffness measurements, in the present work we investigated the effects of the ethanol concentration on the stiffness and evolution of interfacial micropancakes by taking the advantage of quantitative nanomechanical imaging of PF-QNM.

2. EXPERIMENTAL SECTION

2.1 Materials. Highly oriented pyrolytic graphite (HOPG, ZYH grade, NT-MDT, Russia) was freshly cleaved and used as substrate. Ultra-pure water with a conductivity of 18.2 MΩ•cm was obtained by an USF-ELGA Maxima water purification system. Ethanol (≥99.8%, GR), one-use plastic syringes were purchased from Sinopharm Chemical Reagent Co., Ltd. Ethanol solutions with concentration of 0% (pure water), 5%, 10%, 15%, 20% and 25% in volume were prepared in clean glass bottles. The syringes were used to extract and inject liquid. Silicone tubes, a quartz liquid cell and a silicone O-ring provided by Bruker were used to displace and scale the liquid. The new syringes, liquid cell and O-ring were all pre-cleaned with

ethanol and water for three times respectively before use.

2.2 Formation of micropancakes. Micropancakes were prepared on the freshly cleaved HOPG surface by the standard ethanol-water exchange procedure. The details of this procedure have been documented elsewhere.[4] In brief, the freshly cleaved HOPG substrate was firstly exposed to ethanol in a closed AFM liquid cell. And then water was carefully injected into the liquid cell to displace ethanol, after which micropancakes were formed on the HOPG surface. The HOPG surface was first imaged in pure water, and then in ethanol/water solutions (5%, 10%, 15%, 20% and 25% in volume) by directly injecting each of these solutions to replace that in the liquid cell. Particularly, we displaced the last ethanol solution by pure water and then the same area was mapped. After each displacement, the corresponding *in situ* topography and stiffness images were simultaneously mapped. We usually captured the images about ten minutes after the displacement. During each displacement, being careful that large air bubbles should not be allowed to pass through the liquid cell.

2.3 AFM characterization. PF-QNM imaging in fluid was performed on Bruker's Multimode SPM with NanoScope 8 Software and NanoScope V Controller. NPS (Bruker's silicon nitride probes with nominal spring constant of 0.35N/m, tip radius of 10nm) and SNL (Bruker's silicon probes with nominal spring constant of 0.35N/m, tip radius of 2nm) type probes were treated by Plasma Cleaner (HARRICK PLASMA, PLASMA CLEANER PDC-32G) for about one minute beforehand and used immediately to avoid contaminating.

In PF-QNM mode AFM, the deflection sensitivity and spring constant for each cantilever were calibrated using the built-in cantilever calibration, ramp and thermal noise method, respectively. The sample was oscillated at a frequency of 2kHz in the vertical direction with an amplitude of 100nm and scan rate of 0.977Hz. The peakforce setpoint was carefully selected and small loading force (usually 100pN ~ 300pN) was used for imaging. All AFM experiments were performed at ambient conditions. The AFM offline processing system, NanoScope Analysis software was used for morphology and stiffness values measurements and analysis.

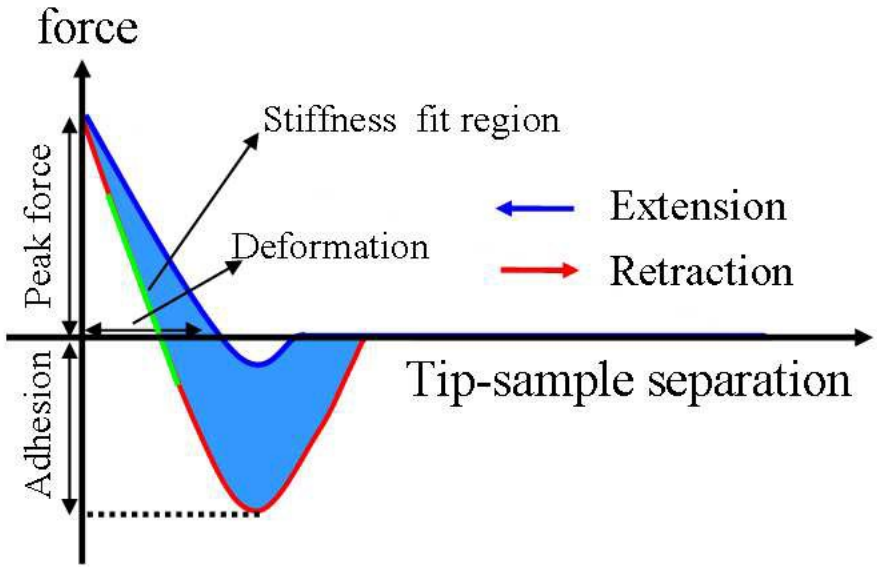

Figure 1. Illustrations of a typical force curve collected by the PF-QNM mode AFM. Different regions of the curve are analyzed and reported in the data acquisition channels of peak force, stiffness, deformation and adhesion.

3. RESULTS AND DISCUSSIONS

3.1 PF-QNM imaging of micropancakes on HOPG surface. Figure 1 illustrates a typical force curve collected by PF-QNM, and different parts of the extension-retraction force curve are indicated to show where the peak force, stiffness, adhesion and deformation are measured through. The height image is obtained from the height correction performed by the feedback loop to keep a constant maximal force (peak force) at each pixel. The stiffness is measured from the slope of the contact region in the retraction curve, the adhesion from the maximal force upon the snap-off of the tip in the retraction curve, and deformation from the extension curve.[40]

The images in Figure 2 were collected from four data acquisition channels simultaneously by PF-QNM on HOPG after the solvent exchange. The observed features are the composites of nanobubble and micropancake (i.e. nanobubble-on-micropancake). The measurements from the height image show that the nanobubbles are 3-46 nm in height and 37-535 nm in lateral diameter while the micropancakes are less than 2 nm in height and from hundreds of nanometers to a few microns laterally. Those morphological properties are consistent with the height measurements by a standard tapping mode.[1, 2, 4, 5, 13-19, 41]

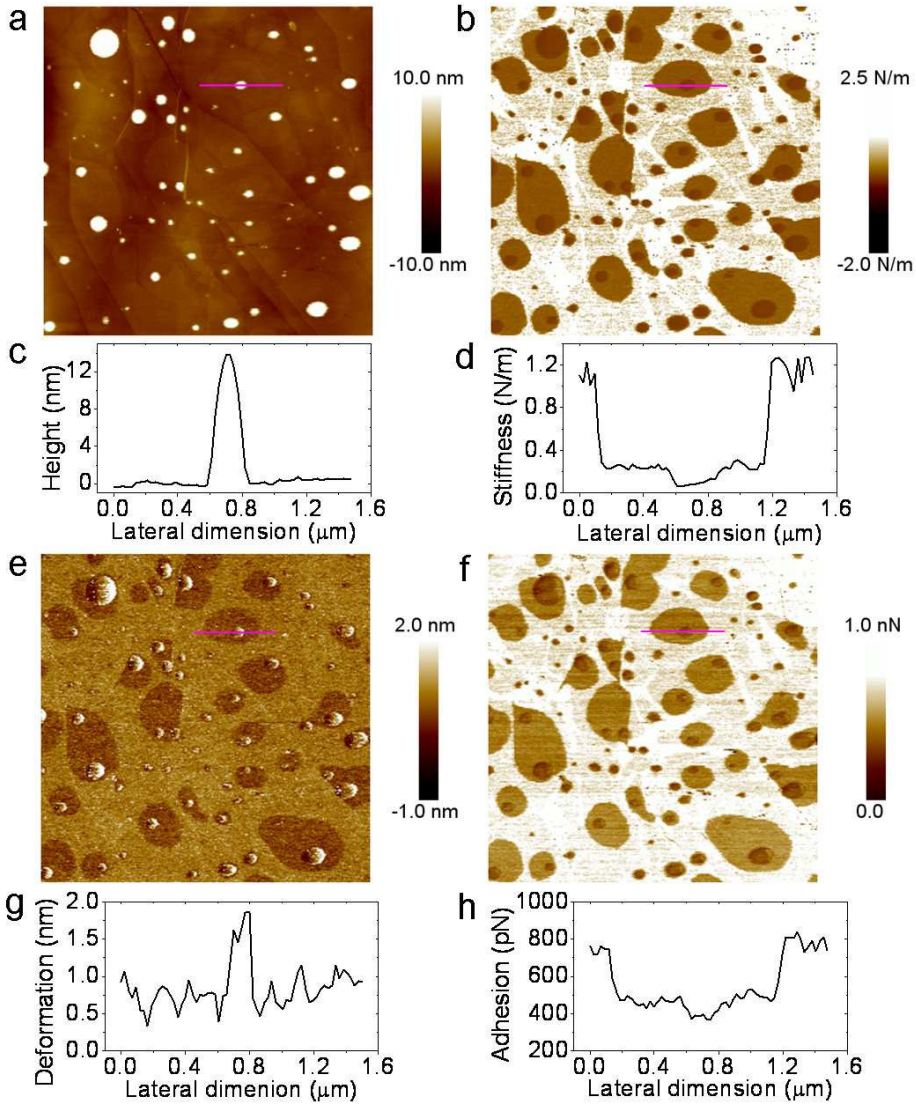

Figure 2. PF-QNM images of micropancakes on HOPG surface immersed in pure water. (a, b, e, f) are respectively the height, stiffness, deformation and adhesion images. (c, d, g, h) are the corresponding profiles from the lines in (a, b, e, f). Scan size: 6μm×6μm, peakforce setpoint: 200pN.

The images of stiffness and adhesion are constructed from two characteristics of the withdraw curves illustrated in Figure 1. The contrast in the stiffness image reflects the relative stiffness of the probed area. In the stiffness image the darker a region is, the softer it is. Figure 2(b, d) clearly show that nanobubbles are relatively softer than micropancakes, and the latter are softer than the substrate. From Figure 2(e, g), we can see that the deformation of nanobubbles is larger than that of micropancakes,

while the deformation of HOPG is between them. Note that the cantilever used here is too soft to measure the deformation of HOPG. The deformation of HOPG here is meaningless. The adhesion image in the same area shows that the adhesion exerted on the tip is stronger on HOPG than on micropancakes or nanobubbles. As nanobubbles, micropancakes and substrate possess distinctive contrast in those images constructed from the retraction curves by PF-QNM, the stiffness image can clearly detect the presence of micropancakes. Below we take advantage of the stiffness image to investigate mechanical properties of micropancakes.

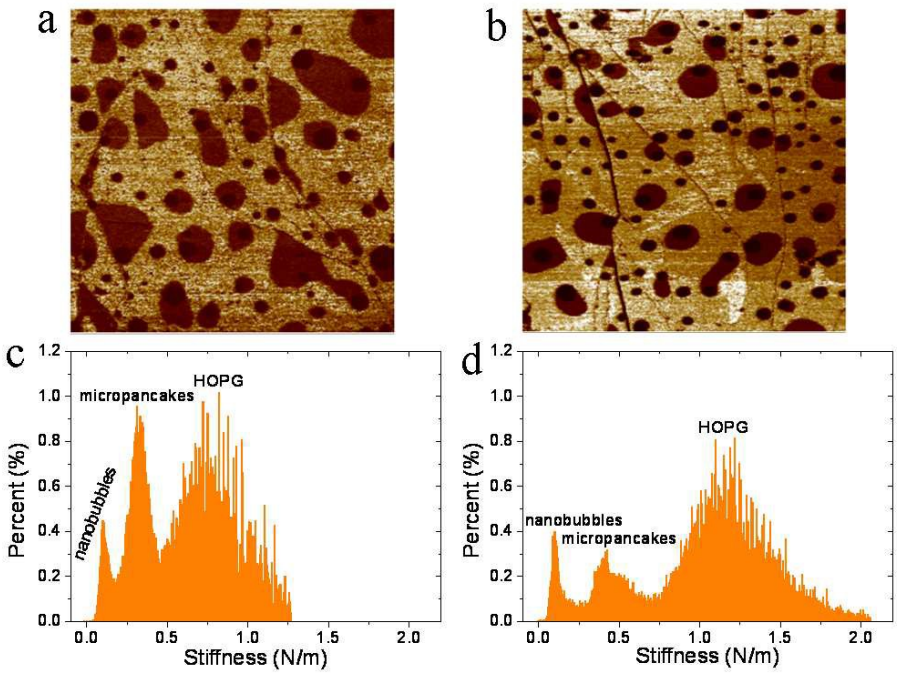

Figure 3. Two representative images showing the measured stiffness of the composites of nanobubble-on-micropancake. (a) and (b) are the stiffness images with scan sizes (a) 5μm×5μm and (b) 8μm×8μm. (c) and (d) are the corresponding histograms. The calibrated spring constants of the cantilevers were 0.32N/m for (a) (c) and 0.34N/m for (b) (d), respectively. Peakforce setpoint: 200pN. Both of images show that nanobubbles are softer than micropancakes.

3.2 The stiffness of micropancakes in pure water. Figure 3 shows two typical stiffness images of nanobubble-micropancake composites and the distribution histograms of the stiffness over the entire examined area. The common feature of the two histograms is that there are three peaks across different range of stiffness. Those three peaks in the histogram are assigned to nanobubbles, micropancakes and substrate, respectively. Under our experimental conditions, the measured stiffness of

micropancakes is between 0.22-0.44N/m in Figure 3c and 0.33-0.58N/m in Figure 3d. The measured stiffness of nanobubbles is 0.06-0.14N/m in Figure 3c and 0.06-0.16N/m in Figure 3d. Here we simply estimate the stiffness from the histograms without corrections for the measurements on the edge or center of nanobubbles. The marginal regions of nanobubbles suffer the edge effect and are always stiffer than the central regions. However, the marginal regions can be ignored here for micropancakes. So we can directly measure the apparent stiffness of micropancakes from the stiffness distribution histograms.

It should be noted that, although the third peak is assigned to HOPG, its value does not have physical meaning. The reason is that the spring constant of the cantilevers that were used in this work is too soft to measure the stiffness of HOPG. A much stiffer type of probe (i.e. TAP525A, with nominal spring constant of 200N/m) is recommended for the most accurate measurement of the stiffness of HOPG.[34] The uncertainty in HOPG stiffness, however, does not influence the results of this work, as the peak just acts as the references for the substrate.

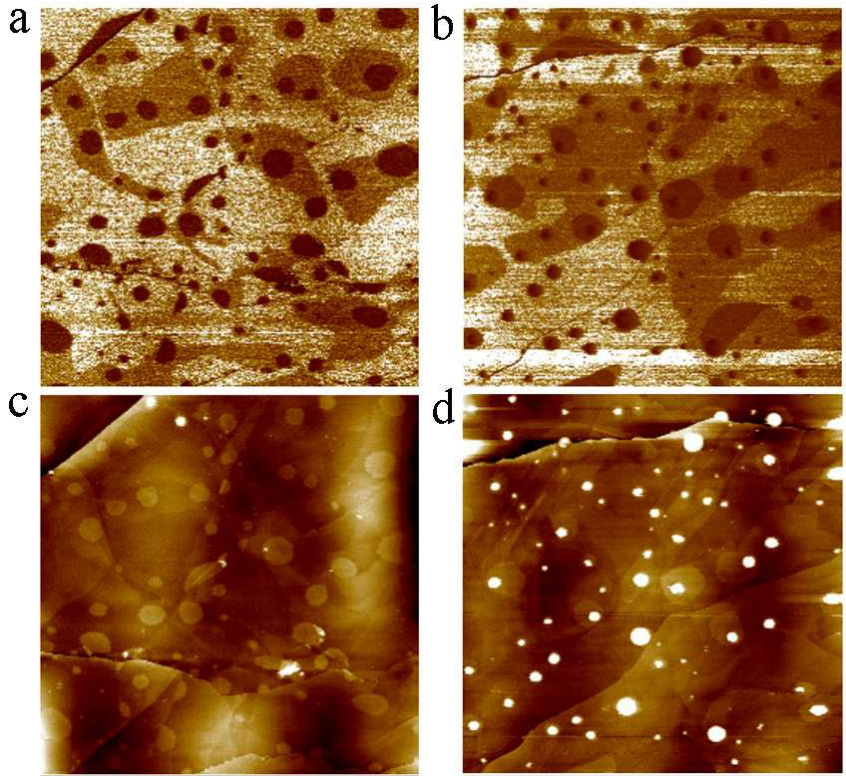

Figure 4. The stiffness and height images of multiple layers of micropancakes. (a, c) Bilayer micropancakes. (b, d) Nanobubble-on-bilayer micropancakes. Scan size: 5μm×5μm**,** peakforce

setpoint: 300pN. The stiffness images show the bottom layer micropancakes (MP-1), the top layer micropancakes (MP-2), nanobubbles (NBs) and HOPG.

In addition to the composites of nanobubble-on-micropancake, there are other forms of micropancakes. Figure 4 shows the height and the stiffness images of bilayer and nanobubble-on-bilayer micropancakes. The height images can only reveal one layer of micropancakes, but the stiffness images clearly shows that there are two layers of micropancakes and that the layer visible in the height images is only the top one (Figure 4c and d). This result demonstrates that the stiffness image is more sensitive than the height image in detection of the multilayers of micropancakes.

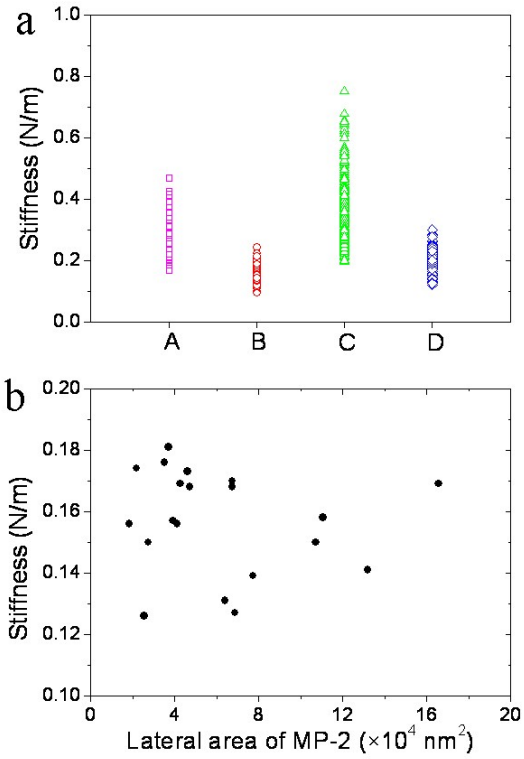

Figure 5. The measured stiffness of multiple layers of micropancakes. (a): A and B are the bottom and top layer of micropancakes in Figure 4a, while C and D are the bottom and top layer of micropancakes in Figure 4b. Each of them contains more than two hundreds of data points. (b): Plot of the measured stiffness versus the lateral area of micropancakes. The data were based on 20 micropancakes on the bottom layer in Figure 4a.

As the contrasts of the bottom and top layers of micropancakes are considerably

different, the measured stiffness values of them are compared as shown in Figure 5. From Figure 5a, we can clearly see that the bottom layers of micropancakes (A and C) are stiffer than the top layer (B and D), which may be due to the stronger substrate effect on the bottom layer than that on the top layer. The substrate effect has been reported in the researches on thin layers of soft materials.[40, 42, 43] Although the absolute value of the measured stiffness of the top and bottom layers of micropancakes may vary from experiment to experiment, the relative value keeps the same order. For example, the order of the measured stiffness is always: NBs < MP-2 < MP-1 < HOPG.

Besides, for bilayer micropancakes, since the bottom layer is irregular in shape and low in contrast and so is difficult to measure the lateral area, we only measured that of the top layer and then plotted the measured stiffness versus the lateral area of the top layer micropancakes. We did not find correlation between the micropancakes stiffness and their lateral sizes, which can be seen from the Figure 5b. Not surprisingly, this is different from the size-dependence of the nanobubble stiffness, because the Laplace pressure might be irrelevant to these flat micropancakes, whereas the Laplace pressure inside the nanobubbles depends on the bubble size,[37] giving rise to different apparent stiffness.[36] It would be interesting to examine the effect of the micropancakes thickness. Unfortunately, we are not able to compare the stiffness difference among micropancakes with different thickness due to the resolution limitation in the height image.

3.3 The stiffness and evolution of micropancakes in ethanol/water solutions. To determine how the stiffness of a single layer of micropancakes is related to the liquid/gas interfacial tension, we examined the effects from ethanol concentration in the liquid. Figure 6 shows the images of micropancakes as the concentration of ethanol/water solutions increases from 0% to 20%. The detailed analysis shows that the measured stiffness of micropancakes decreases with the increase of the ethanol concentration (see Figure 7). The surface tension of the ethanol solution versus the ethanol concentration is also plotted in Figure 7 as a reference. The measured stiffness

of both nanobubbles and micropancakes drop with the increase of ethanol concentration. For 0% to 15% of the ethanol concentration, the measured stiffness of micropancakes and nanobubbles decrease to 46% of the original values. During the process, the micropancakes are always stiffer than nanobubbles, which may illustrate that the surface energy of the liquid-vapor interface is much higher for micropancakes than for nanobubbles in this range of ethanol concentration.

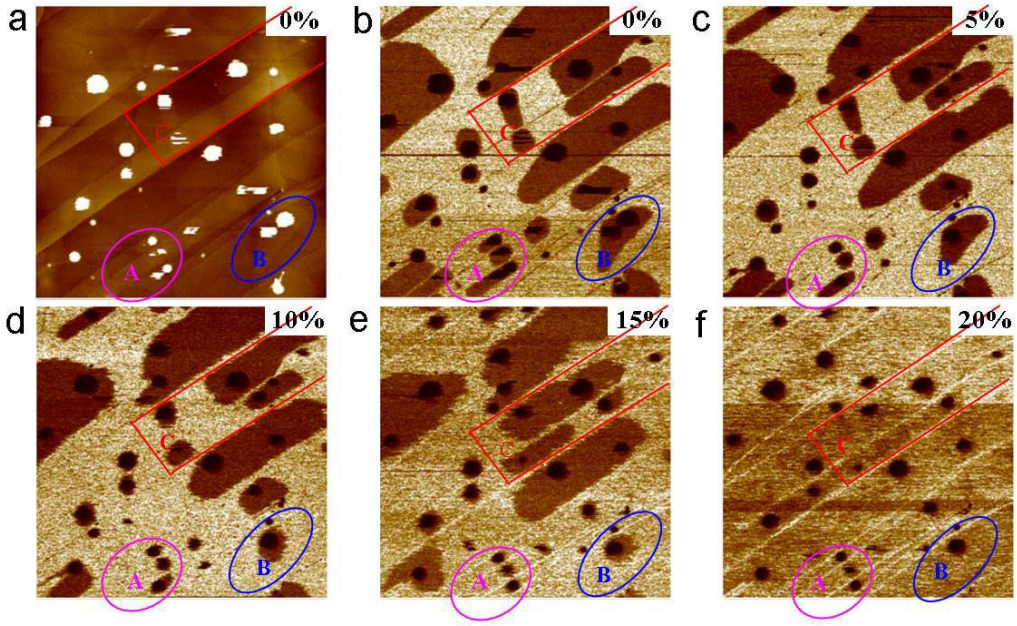

Figure 6. *In situ* PF-QNM imaging of micropancakes in different ethanol/water solutions. (a) Height and (b-f) stiffness images in different ethanol/water solutions. The ethanol concentrations are noted in each image. Scan size: 5μm×5μm, peakforce setpoint: 200pN.

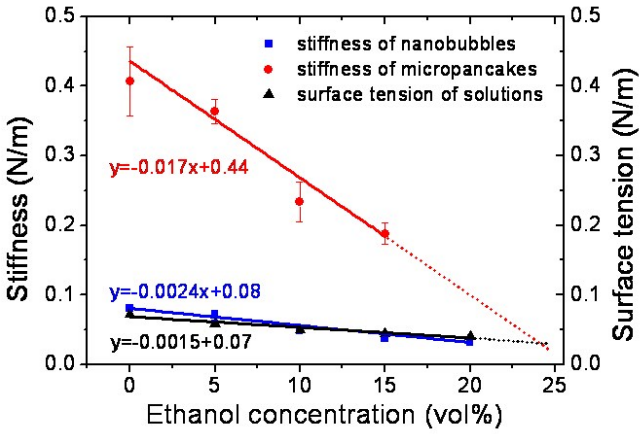

Figure 7. The measured stiffness of micropancakes in ethanol/water solutions. The measured

stiffness of micropancakes decreased dramatically with the increase of the ethanol concentration from 0% to 15% compared to nanobubbles. The linearly fitted lines of the stiffness of micropancakes and the surface tension of the solutions versus the ethanol concentration are extrapolated and they cross at 24% ethanol concentration.

The stiffness images also reveal the change of the lateral size of micropancakes with the ethanol concentration. As showed in Figure 6, the micropancakes in the three typical regions (A, B, C) decrease in their sizes with increasing the ethanol concentration. This result may indicate that a decrease in the saturation of the gas in ethanol/water solutions compared to that in water should account for the reduction in the size of micropancakes.[14] Besides, as for region C, a subtle change occurred when the ethanol concentration changed from 10% to 15%, which might be due to the perturbation from the flow during switching the solutions. However, the most significant change occurs in 20% ethanol solution when all of the micropancakes become invisible in the stiffness image (see Figure 6f).

Table 1 Probability of micropancakes appearance on HOPG surfaces in different ethanol/water solutions. (We totally count 13 experiments. Some concentrations are not tested in some experiments.)

Ethanol concentration	0%	5%	10%	15%	20%	25%
Probability	-	6/8	6/13	2/8	0/10	0/3

More complicatedly, the critical concentration of the ethanol solutions in which micropancakes become invisible may change with the experiments depending on the condition of the formed micropancakes. The probabilities of micropancakes disappearance in different ethanol/water solutions from 0% to 25% are listed in Table 1. Micropancakes remained in 5% for 6 out of 8, in 10% for 6 out of 13, and in 15% for 2 out 8 out of 13 times tests. Among 10 times of 20% solutions and 3 times of 25% solutions, micropancakes were never observed on the surface, either of higher concentrations.

Surprisingly, micropancakes re-appear when the ethanol solution of the critical concentration is replaced with water, as shown in Figure 8. This process of being visible-invisible-visible can be repeated multiple times as long as the liquid is switched between ethanol solution and water. The micropancakes that re-appear in water are at the same location as they are before in the ethanol solution, clearly demonstrating that they may not really removed from the surface or re-form from the nucleation in water, but are solely undetected in the stiffness image collected in the ethanol solution above critical concentration.[13, 14]

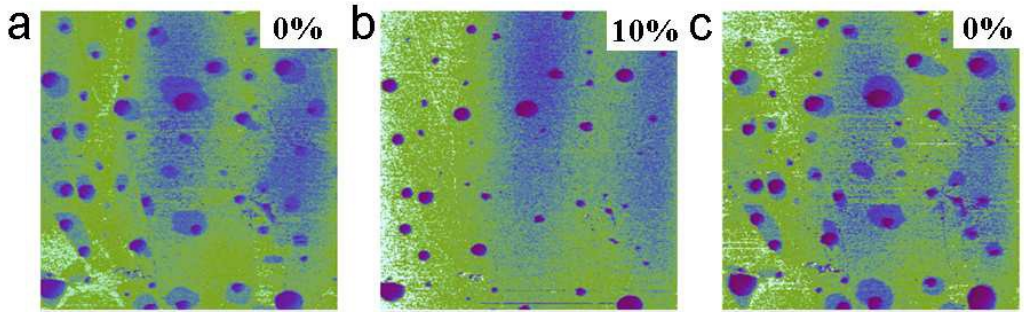

Figure 8. Ethanol effect on the stability of micropancakes. (a), (b) and (c) are the *in situ* stiffness images. Nanobubbles remain while micropancakes are invisible in 10% ethanol/water solution but they re-appear in water. The ethanol concentrations are noted in each image. Scan size: 5μm×5μm, peakforce setpoint: 200pN.

The above results indicate that the micropancakes can sustain a certain ethanol concentration for visualization by the stiffness imaging but become too soft in such ethanol solution to be detected. This is verified by the fact that the stiffness of micropancakes decreased with the increase of the ethanol concentration as is showed in Figure 7. The "come-and-go" behavior indicated that micropancakes are not unstable but should actually be stable in higher concentration ethanol/water solutions than the reported 5%[13, 14]. They were just undetected when the surface tension of solution was reduced under a critical concentration of ethanol. The discrepancy between the stiffness of micropancakes and the surface tension of the solutions decreases with increasing the ethanol concentration. Since they become equal at around the ethanol concentration of 24% according to the extrapolated linearly fitted

lines, we suppose that micropancakes should be able to be stable for detection in the ethanol/water solution with an ethanol concentration as high as 24% (corresponding to the surface tension of ~0.038N/m), which is in contradiction with the experimental results reported before. The gap may be related to some uncontrolled variations on the substrate, the variation in the micropancake thickness or the gas saturation level in the system.

3.4 Further discussions. At present, no measurements have proven unambiguously that micropancakes are indeed gaseous, although degassing effects show that their formation and stability are closely related to the dissolved gases.[13] Some nanobubbles and micropancakes in the literatures were reported to be actually PDMS contaminants.[44, 45] A proposed method to test whether they are gaseous domains or PDMS contaminants is to dry the surface and image the same area in air. If the nanobubbles and micropancakes were gaseous domains, they would disappear when the surface is dry. PDMS contaminants would remain intact after the substrate is taken out from the water.[45] Although how reliable this method can be is yet to be confirmed, we checked our samples anyway by following the proposed method. We found that no nanobubbles or micropancakes were observed after water was removed from the surface. We did not observe residues after removing the liquid and drying the surface. In addition, we compared the results obtained by using plastic and glass syringes in the experiments. Our results showed that there was no considerable difference in the mechanical properties of micropancakes from the experiments using plastic or glass syringes. Furthermore, if we added some PDMS (the material that might cause contamination[44] in water) deliberately to our solution, and after the solvent exchange, we found that PDMS domains were very hard as compared to nanobubbles. The above tests may exclude the possibility of PDMS contamination in our experiments.

Then, how can this work be related to other claimed forms of interfacial gaseous domains? From the AFM height images and profiles of micropancakes, we can see that they have a flat top and a clear boundary. They are limited in thickness (usually several nanometers) but they can spread in lateral dimension from several hundreds

nanometers to even several microns. As we can see from the two dimensional AFM height images that micropancakes are usually like circular or oval, but sometimes they are irregular in shape. The steps on HOPG surface have great effects on the shapes of micropancakes. Very recently Lu et al.[30] observed the pancake-shaped disordered layers and the ordered epitaxial base layers on HOPG surface immersed in oxygen-supersaturated water. However, those pancake-shaped layers and ordered base layers are considerably different in their morphologies from micropancakes investigated in our present study. We believe that more work is required to know whether the micropancakes and those pancake-shaped layers are same in the chemical nature, although they both can form only on crystalline substrates.[16, 30] As the stiffness measurements by PF-QNM provide a sensitive approach to detect the presence of micropancakes and the number of layers, the application of PF-QNM may facilitate the studies on the interactions between micropancakes and other nanoscale features.

4. CONCLUSIONS

We obtained high contrast stiffness images of micropancakes on the HOPG/water interface besides their topographic imaging by using PF-QNM. The nanomechanical imaging clearly revealed nanobubble-on-monolayer micropancakes, bilayer micropancakes, and nanobubble-on-bilayer micropancakes. The stiffness measurements showed that micropancakes in pure water were stiffer than nanobubbles. The addition of ethanol/water solution was found to affect the stiffness and evolution of micropancakes. The stiffness of micropancakes decreased monotonically as the ethanol concentration increased, and the micropancakes became smaller and then invisible above a critical ethanol concentration, but they would recover again after adding pure water, demonstrating the important role of the surface tension in the stiffness, evolution and visualization of micropancakes in ethanol/water solutions. The change of the lateral size of micropancakes with the ethanol concentration and their “come-and-go” behavior indicated their existence in high concentration of ethanol solution, indicating that micropancakes should be stable in a

much higher concentration ethanol/water solution than the previously reported 5%.

■ AUTHOR INFORMATION

Corresponding Author

*E-mail: xuehua.zhang@rmit.edu.au, zhanglijuan@sinap.ac.cn

Notes

The authors declare no competing financial interest.

■ ACKNOWLEDGEMENTS

BYZ is grateful for the inspiring discussions with Prof. Vincent S. J. Craig (Australian National University). The authors thank the support from the Key Laboratory of Interfacial Physics and Technology, Chinese Academy of Sciences, the support from Open Research Project of Large Scientific Facility from Chinese Academy of Sciences: Study on Self-assembly Technology and Nanometer Array with Ultra-high Density. We also thank beamline 08U1A of the Shanghai Synchrotron Radiation Facilities (SSRF) for the sample preparing. We gratefully acknowledge the generous financial support by the National Natural Science Foundation of China (Nos. 11079050, 11290165, 11305252), the National Basic Research Program of China (No. 2013CB932801), the National Natural Science Foundation for Outstanding Young Scientists (no. 11225527), the Shanghai Academic Leadership Program (no. 13XD1404400), 973 project (no. 2012CB825705) and the Knowledge Innovation Program of the Chinese Academy of Sciences (No. KJCX2-EW-W09).

■ REFERENCES

1. Lou, S.-T.; Ouyang, Z.-Q.; Zhang, Y.; Li, X.-J.; Hu, J.; Li, M.-Q.; Yang, F.-J., Nanobubbles on solid surface imaged by atomic force microscopy. *Journal of Vacuum Science & Technology B: Microelectronics and Nanometer Structures* **2000,** 18, (5), 2573-2575.

2. Ishida, N.; Inoue, T.; Miyahara, M.; Higashitani, K., Nano Bubbles on a Hydrophobic Surface in Water Observed by Tapping-Mode Atomic Force Microscopy. *Langmuir* **2000,** 16, (16), 6377-6380.

3. Zhang, X. H.; Zhang, X. D.; Lou, S. T.; Zhang, Z. X.; Sun, J. L.; Hu, J., Degassing and Temperature Effects on the Formation of Nanobubbles at the Mica/Water Interface. *Langmuir* **2004,** 20, (9), 3813-3815.

4. Zhang, X. H.; Maeda, N.; Craig, V. S. J., Physical Properties of Nanobubbles on Hydrophobic

Surfaces in Water and Aqueous Solutions. *Langmuir* **2006,** 22, (11), 5025-5035.

5. Zhang, L.; Zhang, Y.; Zhang, X.; Li, Z.; Shen, G.; Ye, M.; Fan, C.; Fang, H.; Hu, J., Electrochemically Controlled Formation and Growth of Hydrogen Nanobubbles. *Langmuir* **2006,** 22, (19), 8109-8113.

6. Zhang, X. H.; Khan, A.; Ducker, W. A., A nanoscale gas state. *Physical Review Letters* **2007,** 98, (13), 136101.

7. Craig, V. S. J., Very small bubbles at surfaces-the nanobubble puzzle. *Soft Matter* **2011,** 7, (1), 40-48.

8. Seddon, J. R. T.; Lohse, D., Nanobubbles and micropancakes: gaseous domains on immersed substrates. *Journal of Physics: Condensed Matter* **2011,** 23, 133001.

9. Seddon, J. R. T.; Kooij, E. S.; Poelsema, B.; Zandvliet, H. J. W.; Lohse, D., Surface Bubble Nucleation Stability. *Physical Review Letters* **2011,** 106, 056101.

10. Karpitschka, S.; Dietrich, E.; Seddon, J. R. T.; Zandvliet, H. J. W.; Lohse, D.; Riegler, H., Nonintrusive Optical Visualization of Surface Nanobubbles. *Physical Review Letters* **2012,** 109, (6), 066102.

11. Chan, C. U.; Ohl, C.-D., Total-Internal-Reflection-Fluorescence Microscopy for the Study of Nanobubble Dynamics. *Physical Review Letters* **2012,** 109, (17), 174501.

12. Zhang, L.; Zhao, B.; Xue, L.; Guo, Z.; Dong, Y.; Fang, H.; Tai, R.; Hu, J., Imaging interfacial micro- and nano-bubbles by scanning transmission soft X-ray microscopy. *Journal of Synchrotron Radiation* **2013,** 20, (3), 413-418.

13. Zhang, X. H.; Zhang, X.; Sun, J.; Zhang, Z.; Li, G.; Fang, H.; Xiao, X.; Zeng, X.; Hu, J., Detection of Novel Gaseous States at the Highly Oriented Pyrolytic Graphite−Water Interface. *Langmuir* **2007,** 23, (4), 1778-1783.

14. Zhang, X. H.; Maeda, N.; Hu, J., Thermodynamic Stability of Interfacial Gaseous States. *The Journal of Physical Chemistry B* **2008,** 112, (44), 13671-13675.

15. Zhang, L. J.; Zhang, X. H.; Fan, C. H.; Zhang, Y.; Hu, J., Nanoscale Multiple Gaseous Layers on a Hydrophobic Surface. *Langmuir* **2009,** 25, (16), 8860-8864.

16. Zhang, X. H.; Maeda, N., Interfacial Gaseous States on Crystalline Surfaces. *Journal of Physical Chemistry C* **2011,** 115, (3), 736-743.

17. Zhang, L.; Wang, C.; Tai, R.; Hu, J.; Fang, H., The Morphology and Stability of Nanoscopic Gas States at Water/Solid Interfaces. *ChemPhysChem* **2012,** 13, (8), 2188-2195.

18. Hampton, M. A.; Nguyen, A. V., Accumulation of dissolved gases at hydrophobic surfaces in water and sodium chloride solutions: Implications for coal flotation. *Minerals Engineering* **2009,** 22, (9–10), 786-792.

19. Seddon, J. R. T.; Bliznyuk, O.; Kooij, E. S.; Poelsema, B.; Zandvliet, H. J. W.; Lohse, D., Dynamic Dewetting through Micropancake Growth. *Langmuir* **2010,** 26, (12), 9640-9644.

20. Peng, H.; Birkett, G. R.; Nguyen, A. V., Origin of Interfacial Nanoscopic Gaseous Domains and Formation of Dense Gas Layer at Hydrophobic Solid–Water Interface. *Langmuir* **2013,** 29, (49), 15266-15274.

21. Peng, H.; Hampton, M. A.; Nguyen, A. V., Nanobubbles Do Not Sit Alone at the Solid − Liquid Interface. *Langmuir* **2013,** 29, (20), 6123-6130.

22. Dammer, S. M.; Lohse, D., Gas Enrichment at Liquid-Wall Interfaces. *Physical Review Letters* **2006,** 96, (20), 206101.

23. Steitz, R.; Gutberlet, T.; Hauss, T.; Klösgen, B.; Krastev, R.; Schemmel, S.; Simonsen, A. C.;

Findenegg, G. H., Nanobubbles and Their Precursor Layer at the Interface of Water Against a Hydrophobic Substrate. *Langmuir* **2003,** 19, (6), 2409-2418.

24. Doshi, D. A.; Watkins, E. B.; Israelachvili, J. N.; Majewski, J., Reduced water density at hydrophobic surfaces: Effect of dissolved gases. *Proceedings of the National Academy of Sciences of the United States of America* **2005,** 102, (27), 9458-9462.

25. Poynor, A.; Hong, L.; Robinson, I. K.; Granick, S.; Zhang, Z.; Fenter, P. A., How Water Meets a Hydrophobic Surface. *Physical Review Letters* **2006,** 97, (26), 266101.

26. Schwendel, D.; Hayashi, T.; Dahint, R.; Pertsin, A.; Grunze, M.; Steitz, R.; Schreiber, F., Interaction of Water with Self-Assembled Monolayers: Neutron Reflectivity Measurements of the Water Density in the Interface Region. *Langmuir* **2003,** 19, (6), 2284-2293.

27. Lu, Y.-H.; Yang, C.-W.; Hwang, I.-S., Molecular Layer of Gaslike Domains at a Hydrophobic−Water Interface Observed by Frequency-Modulation Atomic Force Microscopy. *Langmuir* **2012,** 28, 12691-12695.

28. Yang, C.-W.; Lu, Y.-H.; Hwang, I.-S., Condensation of Dissolved Gas Molecules at a Hydrophobic/Water Interface. *CHINESE JOURNAL OF PHYSICS* **2013,** 51, (1), 174-186.

29. Lu, Y.-H.; Yang, C.-W.; Hwang, I.-S., Atomic force microscopy study of nitrogen molecule self-assembly at the HOPG–water interface. *Applied Surface Science* **2014,** 304, (0), 56-64.

30. Lu, Y.-H.; Yang, C.-W.; Fang, C.-K.; Ko, H.-C.; Hwang, I.-S., Interface-Induced Ordering of Gas Molecules Confined in a Small Space. *Sci. Rep.* **2014,** 4, 7189.

31. Limbeek, M. A. J. v.; Seddon, J. R. T., Surface Nanobubbles as a Function of Gas Type. *Langmuir* **2011,** 27, (14), 8694-8699.

32. Weijs, J. H.; Snoeijer, J. H.; Lohse, D., Formation of Surface Nanobubbles and the Universality of Their Contact Angles: A Molecular Dynamics Approach. *Physical Review Letters* **2012,** 108, (10), 104501.

33. Peng, H.; Birkett, G. R.; Nguyen, A. V., Progress on the Surface Nanobubble Story: What is in the bubble? Why does it exist? *Adv Colloid Interface Sci* **2014,** in press.

34. Pittenger, B.; Erina, N.; Su, C., Quantitative Mechanical Property Mapping at the Nanoscale with PeakForce QNM. *Bruker application note AN128,Rev. B0* **2012**.

35. Kaemmer, S. B., Introduction to Bruker's ScanAsyst and PeakForce Tapping AFM Technology. *Bruker application note AN133,Rev. A0* **2011**.

36. Zhao, B.; Song, Y.; Wang, S.; Dai, B.; Zhang, L.; Dong, Y.; Lu, J.; Hu, J., Mechanical mapping of nanobubbles by PeakForce atomic force microscopy. *Soft Matter* **2013,** 9, (37), 8837-8843.

37. Wiktoria, W.; Peter, M. S.; Holger, S., The effect of PeakForce tapping mode AFM imaging on the apparent shape of surface nanobubbles. *Journal of Physics: Condensed Matter* **2013,** 25, (18), 184005.

38. Yang, C.-W.; Lu, Y.-H.; Hwang, I.-S., Imaging surface nanobubbles at graphite–water interfaces with different atomic force microscopy modes. *Journal of Physics: Condensed Matter* **2013,** 25, (18), 184010.

39. Zhao, B.; Wang, X.; Wang, S.; Dong, Y.; Zhou, X.; Zhang, L.; Hu, J., Modified Young's Equation with Calibrated Contact Angles for Interfacial Nanobubbles on Graphite with Varied Surface Tensions. *submitted to Scientific Reports*.

40. Rico, F.; Su, C.; Scheuring, S., Mechanical Mapping of Single Membrane Proteins at Submolecular Resolution. *Nano Letters* **2011,** 11, (9), 3983-3986.

41. Walczyk, W.; Schönherr, H., Closer Look at the Effect of AFM Imaging Conditions on the Apparent Dimensions of Surface Nanobubbles. *Langmuir* **2012,** 29, (2), 620-632.

42. Dimitriadis, E. K.; Horkay, F.; Maresca, J.; Kachar, B.; Chadwick, R. S., Determination of Elastic Moduli of Thin Layers of Soft Material Using the Atomic Force Microscope. *Biophysical Journal* **2002,** 82, (5), 2798-2810.

43. Picas, L.; Rico, F.; Scheuring, S., Direct Measurement of the Mechanical Properties of Lipid Phases in Supported Bilayers. *Biophysical Journal* **2012,** 102, (1), L01-L03.

44. Berkelaar, R. P.; Dietrich, E.; Kip, G. A. M.; Kooij, E. S.; Zandvliet, H. J. W.; Lohse, D., Exposing nanobubble-like objects to a degassed environment. *Soft Matter* **2014,** 10, (27), 4947-4955.

45. An, H.; Liu, G.; Craig, V. S., Wetting of nanophases: Nanobubbles, nanodroplets and micropancakes on hydrophobic surfaces. *Adv Colloid Interface Sci* **2014,** in press.

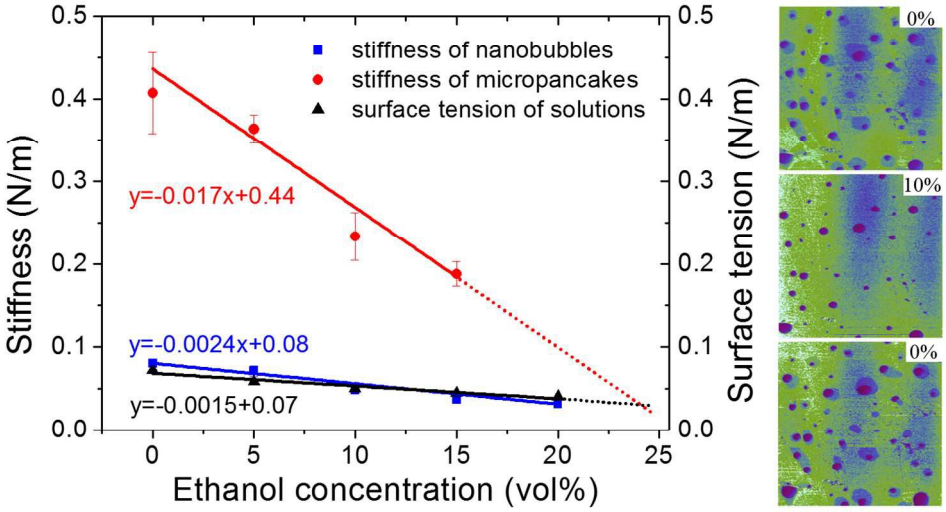

420x242mm (96 x 96 DPI)

Graphical abstract

AFM quantitative nanomechanical imaging revealed the ethanol concentration dependent stiffness, evolution and "go-and-come" behavior of interfacial micropancakes in ethanol solutions.